Architecture dependence of actin filament network disassembly

Laurène Gressin, Audrey Guillotin, Christophe Guérin, Laurent Blanchoin, Alphée Michelot

Architecture Dependence of Actin Filament Network Disassembly

Laurène Gressin,[1] Audrey Guillotin,[1] Christophe Guérin,[1] Laurent Blanchoin,[1,*] and Alphée Michelot[1,*]
[1]Physics of the Cytoskeleton and Morphogenesis Group, Institut de Recherches en Technologies et Sciences pour le Vivant, Laboratoire de Physiologie Cellulaire et Végétale, CNRS/CEA/INRA/UJF, Grenoble 38054, France
*Correspondence: laurent.blanchoin@cea.fr (L.B.), alphee.michelot@cea.fr (A.M.)

SUMMARY

Turnover of actin networks in cells requires the fast disassembly of aging actin structures. While ADF/cofilin and Aip1 have been identified as central players, how their activities are modulated by the architecture of the networks remains unknown. Using our ability to reconstitute a diverse array of cellular actin organizations, we found that ADF/cofilin binding and ADF/cofilin-mediated disassembly both depend on actin geometrical organization. ADF/cofilin decorates strongly and stabilizes actin cables, whereas its weaker interaction to Arp2/3 complex networks is correlated with their dismantling and their reorganization into stable architectures. Cooperation of ADF/cofilin with Aip1 is necessary to trigger the full disassembly of all actin filament networks. Additional experiments performed at the single-molecule level indicate that this cooperation is optimal above a threshold of 23 molecules of ADF/cofilin bound as clusters along an actin filament. Our results indicate that although ADF/cofilin is able to dismantle selectively branched networks through severing and debranching, stochastic disassembly of actin filaments by ADF/cofilin and Aip1 represents an efficient alternative pathway for the full disassembly of all actin networks. Our data support a model in which the binding of ADF/cofilin is required to trigger a structural change of the actin filaments, as a prerequisite for their disassembly by Aip1.

INTRODUCTION

Cells change shape at a microscopic or mesoscopic scale by exerting internal forces based on dynamical actin networks [1]. The turnover of actin is characterized by a rapid, organized, and localized polymerization of actin filaments, followed by their controlled disassembly. However, in an apparent contradiction, actin is a very stable polymer, with a limited capacity to disassemble by itself [1]. The assembly of different types of actin networks in vitro indicates that actin structures can remain stable for long periods of time [2, 3]. Therefore, an essential requirement for cells to perform a rapid actin turnover is to be able to trigger a fast disassembly of aging actin networks, which can only be performed with the contribution of accessory proteins [1, 4].

A central player in actin disassembly is ADF/cofilin, a 13- to 21-kDa protein conserved in all eukaryotes [5]. ADF/cofilin binds to the side of actin filaments and induces important structural changes, which renders them more compliant to bending and twisting [6, 7]. A large body of literature describes how important these structural changes are for the activity of ADF/cofilin. Current models propose that actin filaments fully decorated by ADF/cofilin are stable; however, actin filaments decorated by sub-stoichiometric densities of ADF/cofilin are severed because they accumulate some mechanical stress at the boundaries between bare and ADF/cofilin-decorated segments [6–8].

Severing, by itself, is not sufficient to explain how every actin network can be disassembled in cells (reviewed in [4]). Therefore, other molecular players, including Aip1, have been suggested to cooperate with ADF/cofilin to disassemble actin networks efficiently [9–19]. Aip1 has binding sites for both actin and ADF/cofilin and was recently identified as a crucial factor to destabilize freely fluctuating cofilin-saturated actin filaments [17, 18]. However, (1) how these proteins interact with organized actin networks and how they contribute, individually or together, to their disassembly, have yet to be determined, and (2) how the activities of ADF/cofilin and Aip1 are coordinated at the molecular level to disassemble actin filaments remains unclear.

Here we studied the impact of these families of disassembly factors on actin networks of various architectures. We performed this characterization by using protein micropatterning technologies, which permit the geometrical-control of defined actin organization, combined with total internal reflection fluorescence microscopy and triple-color imaging. We found that the efficiency of actin disassembly factors is dependent on the organization of the filaments. Hence, rather than identifying a unique and general mechanism for the disassembly of actin networks in cells, our work suggests that cells may have alternative pathways for the disassembly of actin networks. In addition, our work at the molecular level indicates a possible unidentified function for ADF/cofilin, as marker to maintain actin filaments or networks in a pre-disassembly state.

RESULTS

ADF/Cofilin-Induced Actin Disassembly Depends on Actin Architecture

We first aimed to characterize the effects of critical components of actin disassembly on different actin architectures. Recently, protein micropatterning has been developed to reconstitute

in vitro, within the same field of observation, the three main cellular actin organizations (i.e., Arp2/3 branched networks, parallel cables, or cables of mixed polarity) [20]. In this study, we micropatterned motifs of Las17 at the surface of coverslips (Figure 1A). Las17 is the homolog of WASP in yeast, a nucleation-promoting factor (NPF) of the Arp2/3 complex able to trigger the formation of actin networks in the presence of a polymerizing mixture containing the Arp2/3 complex and actin [21, 22]. We chose a type of geometry with two parallel bars (of 20-μm length) of Las17 separated by 30 μm. With this motif, branched networks are assembled on the patterns and parallel cables emerged from the free elongation of the filaments away from the patterned areas (Figures 1B and 1C and Movie S1). Cables of mixed polarity are formed between the bars, whereas parallel cables are assembled in other areas. We also pasted on top of the coverslips a 6-mm-thick layer of polydimethylsiloxane (PDMS) pinched with a 6-mm-diameter hole (Figure 1A). PDMS created wells and gave the possibility to bring sequentially additional factors in solution. Actin networks were imaged at the surface of the coverslips with total internal reflection fluorescence microscopy (TIRFM) in order to limit the noise generated by the other fluorescent molecules present in solution [23–25].

When actin assembly from the micropatterned area reached a steady state, we added 2-μM Alexa-488-labeled yeast ADF/cofilin to the reaction mixture (Figure 1D). Although ADF/cofilin interacted with all actin networks, it bound more sparsely on the Arp2/3 networks than on the different populations of cables (Figures 1D and S1A). Binding of ADF/cofilin was correlated with a decrease of the actin fluorescence signal, corresponding to actin disassembly (Figure S1B). The level of disassembly was architecture dependent. Indeed, the actin fluorescence signal after 450 s had decreased more on branched networks than on parallel cables or on cables of mixed polarity (Figures 1D, S1B, and S1C). Experiments performed at different concentrations of ADF/cofilin revealed that even for equivalent binding densities of ADF/cofilin, branched actin networks disassembled better than all the actin cables (Figure S1C). Together, these results indicate a strong dependence of the actin architectures in ADF/cofilin-driven actin network disassembly. ADF/cofilin binding is able to destabilize branched networks but is not sufficient to disassemble bare parallel or antiparallel bundles.

ADF/Cofilin and Aip1 Collaborate to Disassemble Actin Networks Rapidly and Completely

Genetic and biochemical observations indicate that additional disassembly factors, including Aip1, cooperate with ADF/cofilin in vivo [9–11, 13, 18, 26]. Therefore, we tested the synergy between ADF/cofilin and Aip1 on actin network disassembly (Figure 2A). In our experimental system, Aip1 alone was able to bind slowly and homogenously to actin networks (Figures S2A and S2B), but it did not contribute to their disassembly, as revealed by constant fluorescence actin intensity (Figure S2C). The presence of ADF/cofilin on actin networks accelerated the binding of Aip1 (Figures 2B and S2B and Movie S2). In these conditions, Aip1 was able to trigger the disassembly of all actin networks, including parallel and antiparallel actin organizations. Actin network disassembly was very rapid, as >98% of the actin fluorescence signal had disappeared after 20 s. The fluorescence signal of Aip1 was correlated with the amount of ADF/cofilin bound to actin networks during disassembly (Figure 2B). This suggests that the simultaneous presence of actin and ADF/cofilin is required for a fast and efficient binding of Aip1 to actin networks and their disassembly.

We compared the previous experimental situation, where Aip1 disassembles ADF/cofilin bound actin networks (Figures 2 and S2C), with an experimental condition in which ADF/cofilin and Aip1 are introduced simultaneously (Figure S3). While the extent of disassembly is equivalent for both conditions, disassembly occurred over several minutes, on average 15 times more slowly. This suggests that the binding of ADF/cofilin to actin networks is the limiting factor for fast disassembly in this system.

Severing of Actin Filaments Requires the Clustering of a Threshold Number of ADF/Cofilin Molecules

Our observations performed at the whole-network level indicate that ADF/cofilin binding is a pre-requisite for the Aip1-enhanced disassembly of actin structures. Therefore, a deeper understanding of how actin networks are disassembled by the coordination of ADF/cofilin and Aip1 must come from single-filament-scale observations. For that purpose, we updated our TIRFM setup to the observation of single molecules [27]. Calibration of the fluorescence intensity of individual Alexa molecules was performed prior to every experiment, with the measurement of the fluorescence intensity loss of molecules bound to the coverslips during their photobleaching (Figure S4). As a control of our measurement, we compared the average intensity of individual Alexa-labeled actin monomers with the total intensity of actin filaments with different degrees of labeling (data not shown).

We focused our analysis first on the effect of ADF/cofilin on actin filaments. ADF/cofilin binds cooperatively to the side of actin filaments (Figure 3A, white arrows; [6, 8, 28]). At a low concentration of ADF/cofilin (180 nM; Movie S3), the accumulation of ADF/cofilin was slow (about 1.4 molecules • min^{-1}), reaching a maximum of 5 ± 1 molecules, and fragmentation of the filaments rarely occurred (Figures 3A and 3B). At an intermediate concentration of ADF/cofilin (360 nM; Movie S4), it accumulated faster (32 ± 18 molecules • min^{-1}), and fragmentation occurred when the intensity of the ADF/cofilin spots reached a threshold level (Figure 3A, blue arrows; Figure 3B). We quantified the intensity of the spots on the last images before fragmentation, and determined that a number of N_c = 23 ± 8 ADF/cofilins was necessary at the time of severing (Figure 3C). At a high concentration of ADF/cofilin (2 μM), growing actin filaments were fully decorated with ADF/cofilin and were resistant to fragmentation as described previously in the literature (Figure 3A, Movie S5, and [2, 29]).

Actin Filament Severing by ADF/Cofilin Is Polarized

When we performed actin filament severing experiments at an intermediate concentration of ADF/cofilin (360 nM), we noticed that fragmentation events occurred systematically in a polarized manner (Figure 3A, blue arrows). In other words, for every part of the filaments decorated by a stretch of ADF/cofilin, severing systematically occurred at one of the boundaries between decorated and bare sections of the filaments. After severing, one fragment remained practically free of ADF/cofilin at its severed end (<4% of the ADF/cofilin present before severing), while the other

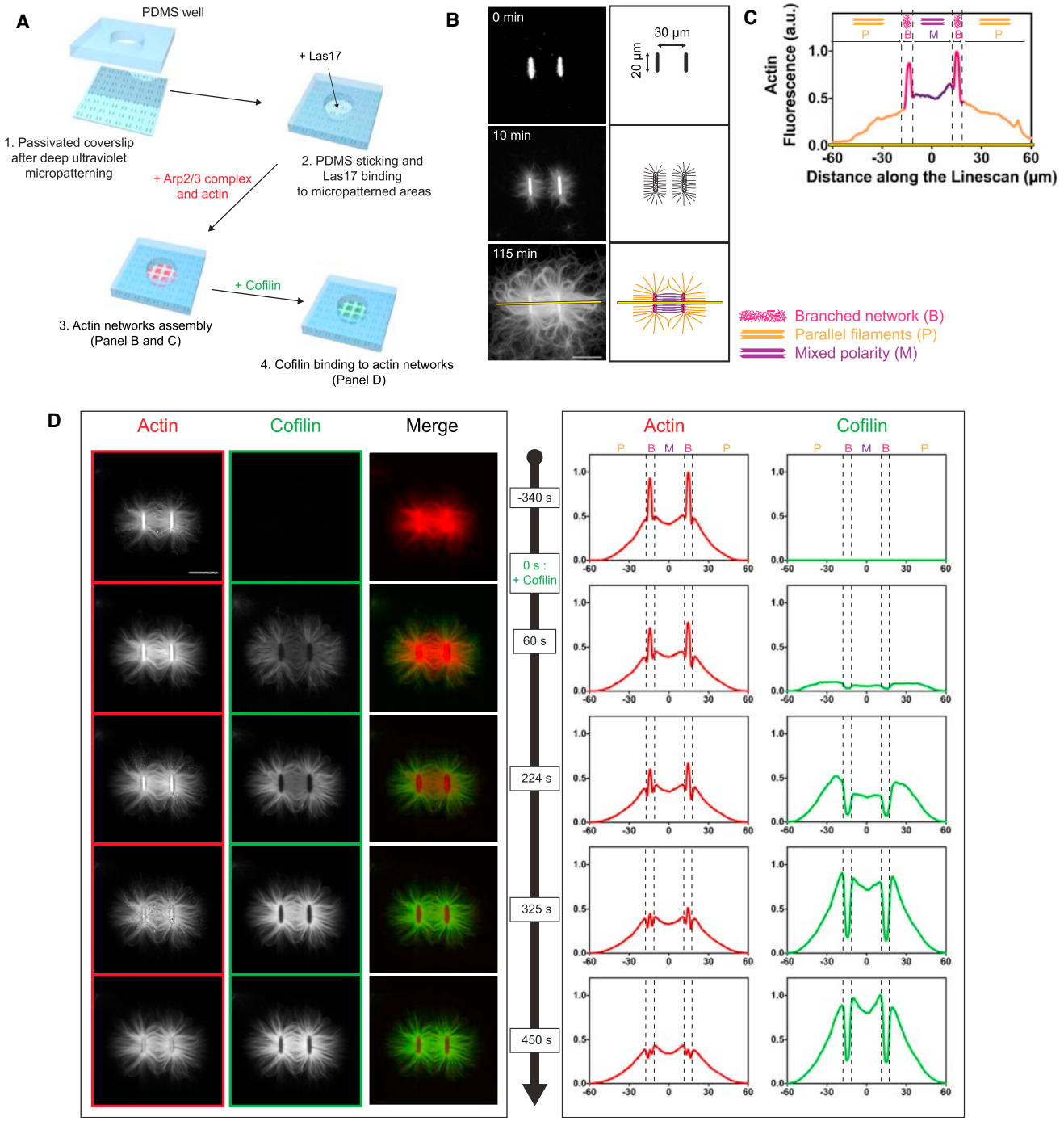

Figure 1. Effect of ADF/Cofilin on Different Actin Network Architectures

(A) Schematic description of the experiment performed in Figure 1.

(B) Left: time course of Alexa-568-labeled actin (2 µM) assembly on Las-17-coated micropatterns in the presence of Arp2/3 complex (20 nM), prior to the addition of ADF/cofilin. Right: color-coded cartoon of actin network architectures.

(C) Quantification of (B). Actin network normalized fluorescence intensity along the yellow linescan indicated in (B) after a 115 min polymerization time is shown.

(D) Left: time course of Alexa-488-labeled ADF/cofilin (2 µM; green) binding to actin networks (red). Right: quantification of actin (red) and ADF/cofilin (green) fluorescence intensities, normalized to their peak intensities.

Scale bars represent 30 µm. See also Figure S1 and Movie S1.

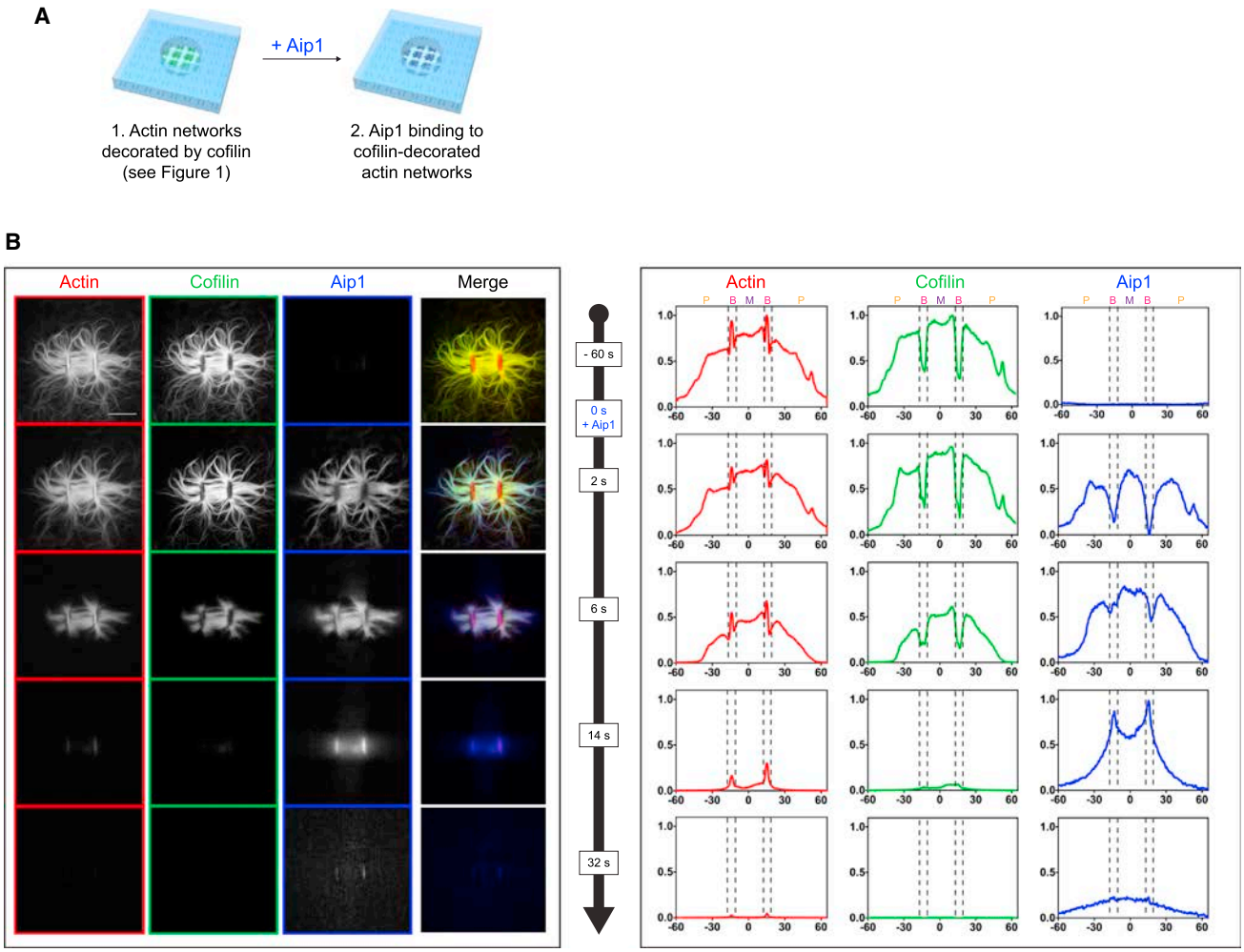

Figure 2. Effect of Aip1 on ADF/Cofilin-Bound Actin Networks

(A) Schematic description of the experiment performed in Figures 2A and 2B and 2C.

(B) Left panels: Time course of Aip1-SNAP-Alexa-647 (1 μM; in blue) binding to ADF/cofilin-decorated actin networks. Right panels: Quantification of actin (in red), ADF/cofilin (in green) and Aip1 (in blue) fluorescence intensities, normalized to their peak intensities. Scale Bar represents 30 μm.

See also Movie S2.

fragment kept the majority of the ADF/cofilin molecules (>88% of the ADF/cofilin present before severing). After many severing events, a large number of fragments decorated with a stretch ADF/cofilin at one of their ends remained on the coverslips (Figure 3D). Photobleaching (FRAP) of the ADF/cofilin stretches showed an absence of fluorescence recovery (Figure 3E). This indicates that ADF/cofilin molecules are bound to actin filaments for long periods of time, without any exchange with the ADF/cofilin molecules in solution [6, 8].

Next, we aimed to determine the nature of the actin filament ends after fragmentation. We imaged the elongation of the fragments, and we observed that actin monomer addition always occurred at the end of the filaments that was left free of ADF/cofilin (Figures 3F and 3G). Altogether, these observations indicate that the fragmentation of actin filaments by ADF/cofilin is a polarized event. After severing, the ADF/cofilin molecules remain on the pointed end of the new fragments, whereas the barbed ends are bare and free to elongate.

The Number of ADF/Cofilin Bound to Actin Regulates Aip1-Induced Disassembly

We focused next on the effect of Aip1 at the filament scale. We polymerized actin filaments in the presence of different concentrations of ADF/cofilin for 5 min, and then injected 1-μM Aip1 (Figure 4A). Our results indicate that the number of ADF/cofilin molecules that accumulated along the actin filaments modulated the activity of Aip1. In the absence or at a low concentration of ADF/cofilin, Aip1 did not show any effect, and ADF/cofilin stretches remained stable along the actin filaments over long periods of time (>2 min) (Figures 4B and 4C and Movie S6). At an intermediate concentration of ADF/cofilin, Aip1 did not catalyze the severing reaction (Figure 4D). However, when a severing event occurred, we observed a progressive decrease of the number of ADF/cofilins bound at the pointed ends of the actin fragment (Figures 4B and 4C and Movie S7). Since the ADF/cofilin stretches are stable in the absence of Aip1, this decrease indicates that Aip1 unloads several ADF/cofilin molecules from

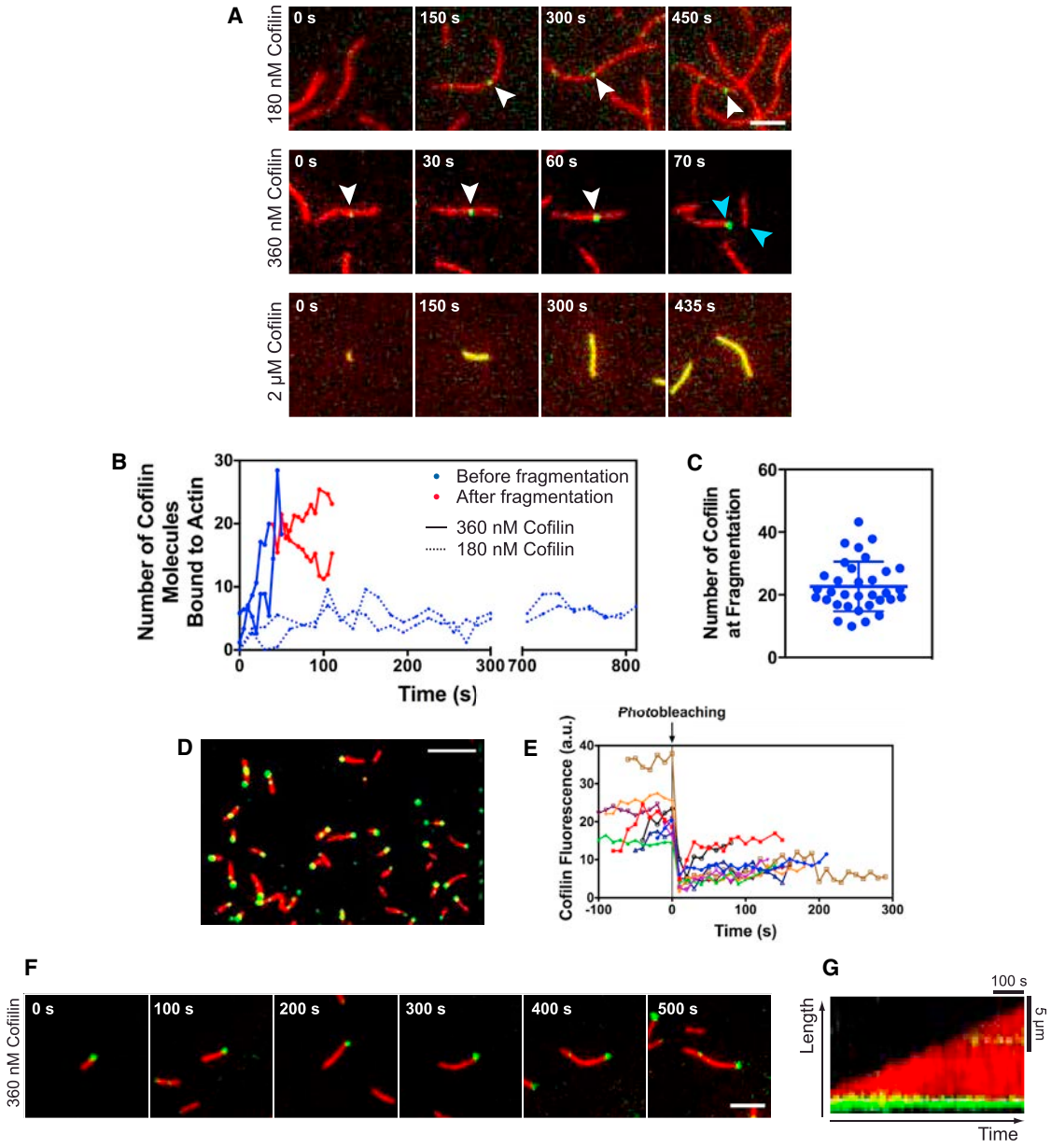

Figure 3. Quantitative Measurement of ADF/Cofilin Accumulation along the Side of Individual Actin Filaments

(A) Time course of Alexa-488-labeled ADF/cofilin (green) binding to individual actin filaments (800 nM; red), at the indicated concentrations. White arrowheads show representative examples of ADF/cofilin cooperative binding to actin filaments. Blue arrowheads show a representative example of a severing event, where ADF/cofilin molecules remain mainly on one end of the fragments. The scale bar represents 5 μm.

(B) Quantification of (A). A time course of four representative molecular accumulations of ADF/cofilin along actin filaments for 180 nM (dotted lines) or 360 nM (continuous lines) of ADF/cofilin is shown. Curves are plotted in blue prior to fragmentation and in red after fragmentation occurred.

(C) Quantification of (A) and (B). Distribution of the number of ADF/cofilin molecules bound to actin filaments prior to severing is shown (23 ± 11 molecules; n = 46). Error bars indicate the SD.

(D) Representative field of observation after many fragmentation events with 360-nM ADF/cofilin. The scale bar represents 10 μm.

(E) Fluorescence recovery after photobleaching (FRAP) of ADF/cofilin accumulations after severing.

(F) Time course of actin filament elongation after severing. The scale bar represents 5 μm.

(G) Kymograph of (D), plotted along the axis of the filament.

See also Figures S2–S4 and Movies S3, S4, and S5.

the severed ends or triggers the disassembly of a short part of the filament. Aip1 showed its most dramatic effect at a high concentration of ADF/cofilin, where it was very effective in disassembling actin filaments fully decorated with ADF/cofilin (Figure 4B and Movie S8). Disassembly was complete within 4 s. Overall, these results were confirmed with a measurement of

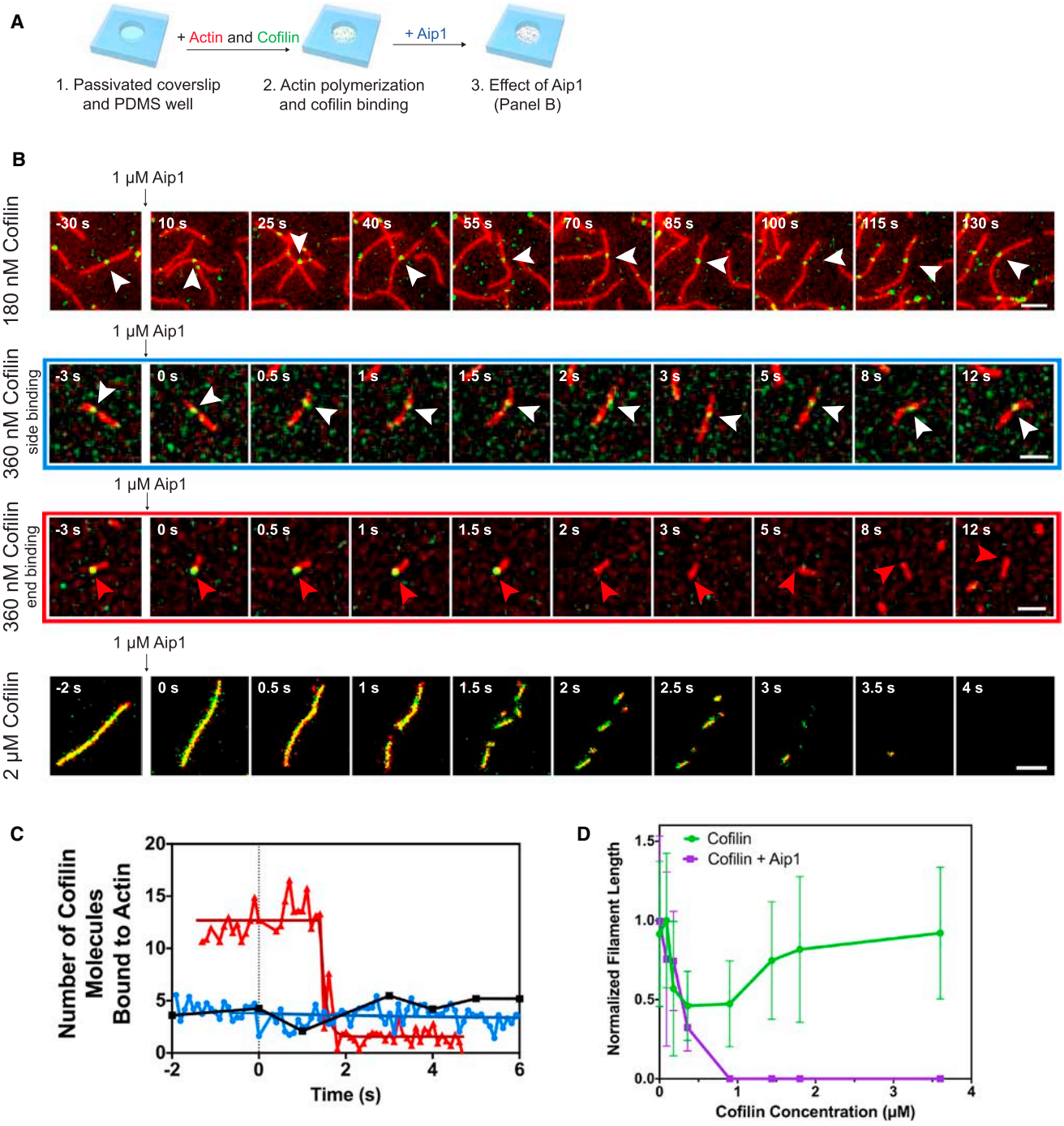

Figure 4. Effect of Aip1 on Individual ADF/Cofilin-Bound Actin Filaments

(A) Schematic description of the experiment performed in Figure 4.

(B) Time course of Aip1's (1 μM) effect on individual actin filaments (800 nM; red) decorated with various amounts of ADF/cofilin (green). White arrowheads track representative examples of ADF/cofilin stretches bound to the side of actin filaments (non-severing events). Red arrowheads track representative examples of ADF/cofilin stretches bound to the pointed end of actin filaments (subsequent to a severing event). Scale bars represent 5 μm.

(C) Quantification of (B). A time course of three representative ADF/cofilin stretches along actin filaments at 180 nM (black curve) and 360 nM (red and blue curves) of ADF/cofilin after injection of Aip1 is shown. Clusters of ADF/cofilin are observed either before (blue curve) or after (red curve) the fragmentation occurred. Fluorescence signal decrease of end-binding ADF/cofilin clusters were fitted with a monoexponential decay (T_{decay} = 1.3 ± 1.1 s; n = 14).

(D) Quantification of the filament lengths as a function of ADF/cofilin concentration, in the presence of 800 nM actin alone or in the presence of 800 nM actin and 1 μM Aip1, normalized to the maximum values. Error bars indicate the SD.

See also Figures S4 and S5 and Movies S6, S7, and S8.

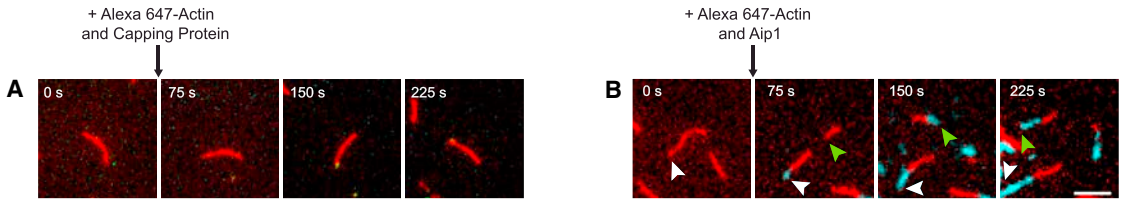

Figure 5. Actin Filament Elongation Assay in the Presence of ADF/Cofilin and Aip1

(A) Time course of Alexa-568-actin filament (800 nM; red) elongation in the presence of 360 nM ADF/cofilin after injection of 800 nM Alexa-647-actin monomers (blue) and 20 nM capping protein.

(B) Time course of Alexa-568-actin filament (800 nM; red) elongation in the presence of 360 nM ADF/cofilin after injection of 800 nM Alexa-647-actin monomers (blue) and 1 μM Aip1. The scale bar represents 5 μm.

the average length of the actin filaments. The length of the filaments was comparable for concentrations of ADF/cofilin up to 300 nM, whether Aip1 was present in solution or not. However, the length of the filaments rapidly dropped to sizes below the diffraction limit of our microscope for higher concentrations of ADF/cofilin in the presence of Aip1 (Figure 4D).

The effect of Aip1 on ADF/cofilin-bound actin filaments was dose dependent. Indeed, a low concentration of Aip1 (5 nM) changed the kinetic of actin filament disassembly, but not its extent (Figure S5). Slower disassembly allowed us to track the fate of the disassembling filaments. We observed a frequent severing of the filaments until they were too short to be detected, but we did not convincingly observe any fast depolymerization or bursting of the filaments ends as previously reported [18, 30].

We also performed these experiments with various concentrations of Alexa-labeled Aip1, but we failed to detect any interaction of Aip1 with either ADF/cofilin or single actin filaments prior to disassembly (data not shown). This suggests that a very transient interaction of a low number of Aip1 molecules with ADF/cofilin and/or actin is sufficient to trigger the disassembly of the filaments.

Effect of ADF/Cofilin and Aip1 on Actin Filaments Barbed Ends

In the past, a number of genetic and biochemical observations suggested that ADF/cofilin and Aip1 may have the ability to inhibit the elongation of actin filament barbed ends [11, 31, 32]. However, whether these two proteins are sufficient for this effect remains controversial [17, 18, 33]. A difficulty in detecting such an inhibition arises from the simultaneous efficiency of ADF/cofilin and Aip1 in disassembling filaments into non-polymerizable low-molecular-weight species [34]. Therefore, in this study, we could only test barbed-end capping on Alexa-568-actin filaments pre-assembled in the presence of an intermediate concentration of ADF/cofilin (Figures 5A and 5B). Although simultaneous addition of Alexa-647-actin monomers and 20-nM capping protein induced a rapid and strong capping of the Alexa-568-actin filaments (Figure 5A), simultaneous addition of Alexa-647-actin monomers and 1-μM Aip1 (which corresponds roughly to the concentration of Aip1 in cells [32]) did not induce barbed-end capping, even at sites where fragmentation events occurred (Figure 5B). In these conditions, the simultaneous presence of ADF/cofilin and Aip1 did not modify the elongation rate of actin filaments (data not shown).

In vivo, capping protein sterically limits the barbed-end elongation of actin filaments before they are disassembled. Two publications questioned a potential inhibitory effect of barbed-end capping for the fast disassembly of actin filaments, leading to contradictory results [30, 33]. We tested this hypothesis in our system by adding capping protein to a solution of actin filaments polymerizing in the presence of 2-μM Alexa-488-cofilin (Figure 6). We verified that actin filament elongation was interrupted before addition of Aip1. Actin filaments disassembled in the presence of capping protein and in its absence, showing that barbed-end capping is not an obstacle to filament disassembly.

DISCUSSION

In this study, we have detailed the interplay between ADF/cofilin and Aip1 to disassemble actin, both at the filament scale and at the level of the different cellular actin organizations.

Actin Disassembly and Network Architecture Specificities

Several lines of evidence indicate that in vivo, disassembly factors act on different actin networks with variable efficiency and provide disassembly rates over different time scales. One example comes from observations in yeast, which contain three types of actin organizations. At the cell cortex, endocytic actin patches are composed of Arp2/3 branched networks. Their average lifetime is about 15 s, with a disassembly phase of about 6 s [35–37]. Inside the cell body, actin cables are composed of short parallel actin filaments, mostly of identical orientations [38]. Actin cables are very dynamic and disappear within seconds [36, 39]. At the division site, a cytokinetic ring is composed of short parallel actin filaments, with identical orientations or mixed polarities depending on the stage of cell division [40]. Most recent works indicate turnover values for the ring ranging from 11 s to several minutes [36, 41, 42]. ADF/cofilin and Aip1 are mainly detected on actin patches, indicating an apparent affinity of these proteins that is higher for branched networks than for linear networks [10, 43]. Interestingly, depletion of Aip1 in budding yeast partially relocalizes ADF/cofilin from actin patches to cables. In these mutants, decoration of actin cables by ADF/cofilin is correlated with their stabilization [10, 13].

These cellular observations indicate the existence of important rules linking actin structural organization with its disassembly. Previous works have demonstrated that the effects of actin binding proteins are not necessarily the same when they interact with

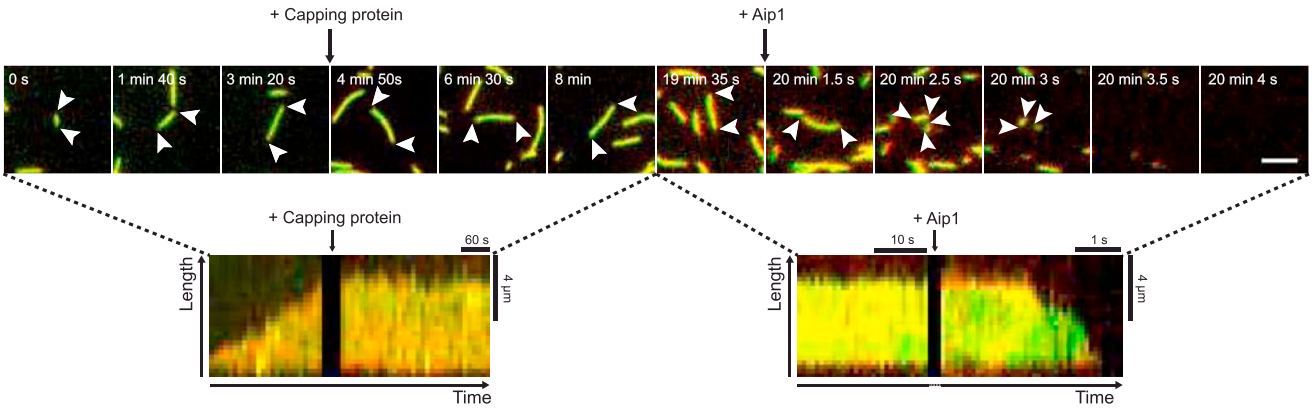

Figure 6. Effect of ADF/Cofilin and Aip1 on Actin Filaments Blocked by Capping Protein

Top: time course of actin filament (800 nM) elongation in the presence of 2-μM Alexa-488-ADF/cofilin for 4 min, followed by a first injection of 20-nM capping protein for 16 min and a second injection of 1-μM Aip1. The scale bar represents 5 μm. Bottom: kymograph of the experiment plotted along the axis of a representative actin filament.

individual actin filaments or with different types of actin architectures [36, 44]. Therefore, we hypothesized that network geometrical organization could be one of the key parameters to explain how actin disassembly is regulated in cells. Our results now indicate that ADF/cofilin binding to actin is architecture dependent (Figures 1 and 7A). ADF/cofilin can disassemble branched actin networks but is unable to disassemble parallel cables or cables of mixed polarity. A probable explanation arises from the fact that ADF/cofilin's binding accelerates the debranching of the Arp2/3 complex [45, 46], which is expected to induce a progressive loss of structural integrity of branched networks and their faster dismantling (Figure 7A). However, even for branched actin networks, ADF/cofilin is unable to fully convert actin networks into actin monomers. At steady state, a population of fragments loaded with ADF/cofilin remains stable over long periods of time (Figures 1 and 7A). Moreover, on parallel cables or cables of mixed polarity, ADF/cofilin induces only a marginal disassembly and these structures remain highly decorated by ADF/cofilin. In previous studies, this effect has been proposed to have a physiological relevance for the stabilization of some cellular actin structures [2]. Our work now suggests that ADF/cofilin loading on to actin filaments could also be an essential prerequisite for Aip1-mediated actin disassembly. From these results, we can now propose a simple interpretation of the *aip1Δ* phenotypes observed in cells. Our explanation is that ADF/cofilin-loaded actin cables become unable to disassemble in the absence of Aip1, whereas actin patches may still use debranching as an efficient alternative for disassembly.

New Insights about the Interaction of ADF/Cofilin with Actin Filaments

At the filament scale, we found unexpected properties of ADF/cofilin's interaction with actin. Our single-molecule detection imaging capacity enabled us to quantify the number of ADF/cofilin molecules bound to the side of actin filaments in real time. We demonstrate that severing induced by ADF/cofilin is a much more efficient and regulated mechanism than previously thought. We measured that a minimal cluster of 23 ADF/cofilin molecules along an actin filament is necessary for efficient severing (Figures 3 and 7B). A large body of literature details how the binding of ADF/cofilin to actin filaments modifies their ultra-structural and -mechanical properties [6, 7, 47, 48]. We propose that a threshold number of 23 ADF/cofilin molecules in a cluster is required to trigger a conformational change on actin filaments and to provide enough mechanical stress for their fragmentation (Figure 7B).

Moreover, the dissymmetry in severing suggests that the mechanical stress created by the ADF/cofilin stretches is polarized. These results are in line with observations performed at the ultrastructural level. High-speed atomic force microscopy has recently revealed that the helical pitch of ADF/cofilin-decorated actin filaments is 25% shorter compared to bare filaments [49]. This conformational change is only propagated to the neighboring bare segments on the pointed end side of the clusters, but not on the barbed-end side. Consequently, this study found that ADF/cofilin clusters only grow toward the pointed end of actin filaments. This observation explains why clusters do not accumulate more ADF/cofilin molecules at the pointed ends of the fragments after a successful severing event in our experiments.

A Step Forward in our Understanding of Actin Filament Disassembly by ADF/Cofilin and Aip1

ADF/cofilin and Aip1 work in tandem to fully disassemble any type of actin organization. In this study, we used triple-color single-molecule imaging to dissect the effect of Aip1 on individual actin filaments decorated by variable numbers of ADF/cofilin molecules (Figure 4). We have integrated our results into a model based on the observation that Aip1 requires the same minimal stretch of 23 ADF/cofilins bound to actin filaments to disassemble them efficiently (Figure 7B). We propose that Aip1-stimulated disassembly requires the conformational change on actin filaments induced by a minimal local density of ADF/cofilin. In this model, actin filaments or higher-ordered organizations fully decorated by ADF/cofilin become ideal substrates for Aip1.

How destabilization of actin filaments by Aip1 occurs remains to be determined at the structural level, but an interesting hypothesis is that actin filaments could disassemble through

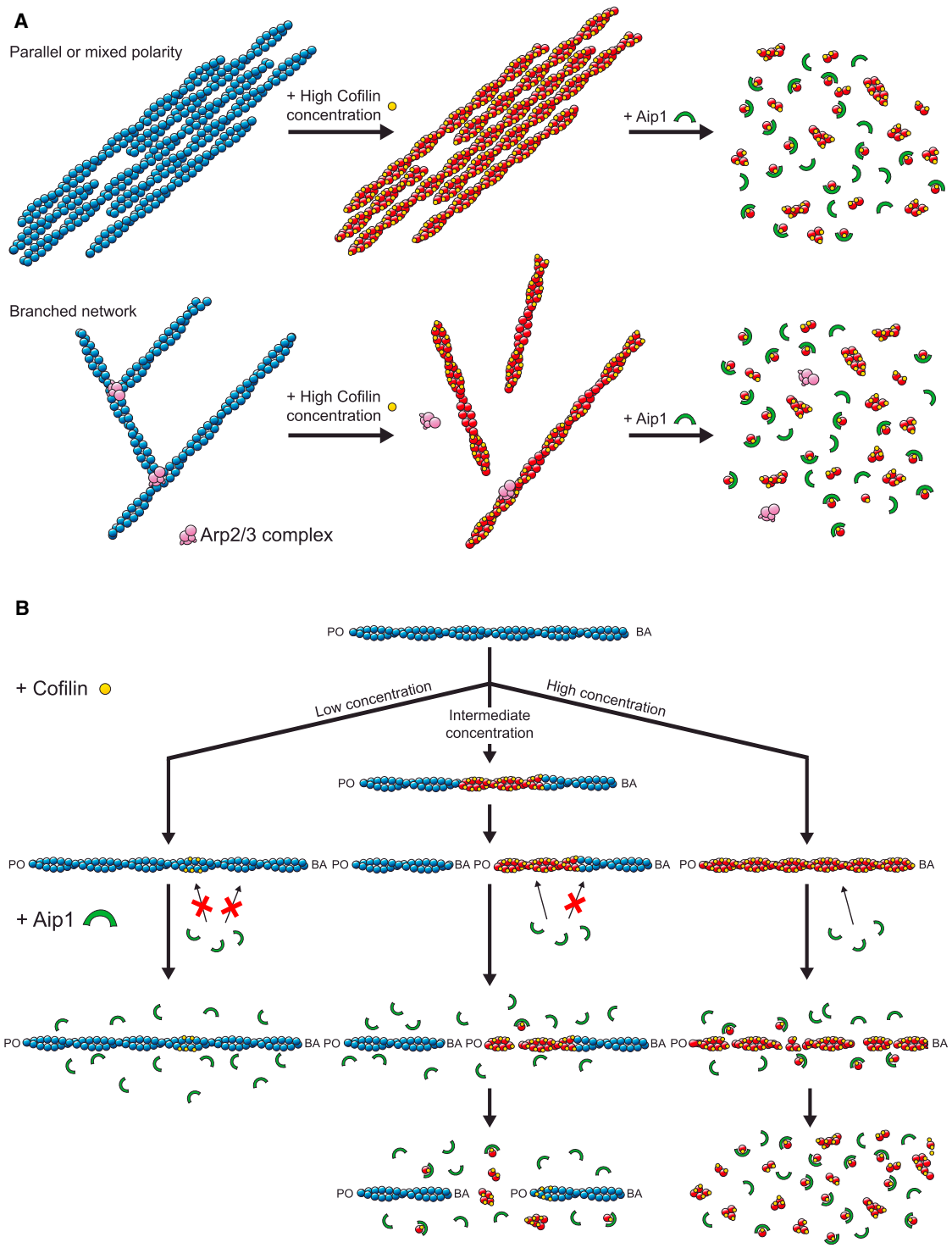

Figure 7. Models for the Disassembly of Actin by ADF/Cofilin and Aip1

(A) Disassembly at the whole-network scale: architecture dependence. In this model, binding of ADF/cofilin to actin cables does not trigger their disassembly, but switches actin filaments (blue filaments) to a pre-disassembly state (red filaments) (top). However, ADF/cofilin has an important effect for the dismantling of branched networks, through its de-branching activity (bottom). For all actin networks, presence of Aip1 turns these stable ADF/cofilin-decorated structures into unstable assemblies, prone to stochastic disassembly.

(B) Severing and disassembly at the single-filament scale. In this model, binding of ADF/cofilin needs to reach a threshold level of 23 molecules to trigger a conformational change of the filaments (represented by a change in their color, from blue to red). At a low concentration of ADF/cofilin (left), the threshold level is not reached. At an intermediate concentration of ADF/cofilin (center), actin filaments decorated by sub-stoichiometric densities of ADF/cofilin but with N > 23

cooperative strand separation [30]. Such mechanism was described to induce in vitro shortening of actin filaments by bursts at their ends. In our work, we have not been able to detect any bursting event from the ends of the filaments and capping protein was not an inhibitor of disassembly. Therefore, our results do not support the existence of any end bursting for the fast disassembly of yeast actin filaments, although we do not rule out the possibility that bursting could come from some isoform specificity. Nevertheless, the fact that Aip1 is sufficient in our system to induce a disassembly of actin networks at cellular rates does not support the necessity of any end bursting to describe the synergy between ADF/cofilin and Aip1.

EXPERIMENTAL PROCEDURES

Protein expression, purification, and labeling are detailed in the Supplemental Experimental Procedures.

Sample Preparation

Glass Cleaning

Glass slides and coverslips were cleaned by sonication at room temperature for 15 min in 1 M aqueous NaOH and for 15 min in ethanol. They were extensively rinsed with deionized Milli-Q (Millipore) filtered water after each sonication step and were eventually dried and stored for up to 2 weeks at room temperature.

Glass Passivation

Slides and coverslips were plasma treated for 3 min at 80–90 W (Femto; Diener Electronic) and immediately incubated with a passivation agent. For the micropatterning-based experiments, slides and coverslips were incubated with 0.1 mg/ml Poly(L-lysine)-poly(ethyleneglycol) in 10 mM HEPES (pH 7.4) for 30 min at room temperature, washed gently in water, dried, and stored at 4°C for up to 1 week. For the single-filament-scale experiments, slides and coverslips were incubated with 1 mg/ml Silane-PEG 5K in a solution of ethanol complemented with 0.1% HCl for 18 hr at room temperature under gentle shaking, washed extensively in ethanol and water, dried, and stored at 4°C for up to 1 week.

PDMS Wells

PDMS wells were prepared by mixing 10 g of DMS (Sylgard 184 Silicone Elastomer; Dow Corning) for each gram of curing agent. The mixture was degassed for a minimum of 45 min, spread into 7-mm-thick layers, and heated at 100°C until it hardened (i.e., for about 20 min). PDMS was cooled down, cut to appropriate shapes, and stuck to the coverslips. An additional cover of PDMS was placed on top of the wells to avoid evaporation.

Las17 Micropatterning

Surface patterns were created by the deep UV micropatterning method as previously described [20, 50]. 10 μl of a 200-nM solution of Las17 in its purification buffer was incubated with the micropatterened areas inside the wells for 15 min at 4°C.

Actin Assembly

Yeast actin, rabbit actin, and labeled rabbit-muscle actin were mixed in G buffer (5 mM Tris-HCl [pH 8], 0.2 mM ATP, 0.1 mM $CaCl_2$, 0.5 mM DTT, and 1 mM NaN_3) to a final ratio of 1:4 (rabbit actin:yeast actin), with an overall 10% labeling percentage. Actin polymerization was initiated by mixing the proteins of interest in F buffer (10 mM imidazole-HCl [pH 7.0], 75 mM KCl, 1 mM EGTA, 1 mM ATP, 1 mM $MgCl_2$, 70 mM DTT, 2.5 mg/ml glucose, 15 μg/ml catalase, 70 μg/ml glucose oxidase, 0.1% BSA, and 0.3% methylcellulose).

TIRF Microscopy and Data Analysis

Time course of actin assembly was acquired on a Nikon Eclipse Ti microscope, equipped with a 60× objective and an Evolve EMCCD camera (Photometrics) using Metamorph v.7.7.10.0. Data were analyzed with ImageJ v.1.48 and plotted with GraphPad Prism 6.

SUPPLEMENTAL INFORMATION

Supplemental Information includes Supplemental Experimental Procedures, five figures, and eight movies and can be found with this article online at http://dx.doi.org/10.1016/j.cub.2015.04.011.

ACKNOWLEDGMENTS

The authors acknowledge Shirin Hashem for her comments and corrections on the manuscript. L.G. was supported by an Irtelis PhD fellowship (CEA). This project was supported by Labex GRAL and ANR grant number ANR-12-BSV5-0014 (Contract) to L.B. and number ANR-14-CE11-0011-01 (DiANe) to A.M.

Received: January 1, 2015
Revised: March 6, 2015
Accepted: April 8, 2015
Published: April 23, 2015

REFERENCES

1. Blanchoin, L., Boujemaa-Paterski, R., Sykes, C., and Plastino, J. (2014). Actin dynamics, architecture, and mechanics in cell motility. Physiol. Rev. *94*, 235–263.
2. Michelot, A., Berro, J., Guérin, C., Boujemaa-Paterski, R., Staiger, C.J., Martiel, J.L., and Blanchoin, L. (2007). Actin-filament stochastic dynamics mediated by ADF/cofilin. Curr. Biol. *17*, 825–833.
3. Achard, V., Martiel, J.L., Michelot, A., Guérin, C., Reymann, A.C., Blanchoin, L., and Boujemaa-Paterski, R. (2010). A "primer"-based mechanism underlies branched actin filament network formation and motility. Curr. Biol. *20*, 423–428.
4. Brieher, W. (2013). Mechanisms of actin disassembly. Mol. Biol. Cell *24*, 2299–2302.
5. Poukkula, M., Kremneva, E., Serlachius, M., and Lappalainen, P. (2011). Actin-depolymerizing factor homology domain: a conserved fold performing diverse roles in cytoskeletal dynamics. Cytoskeleton (Hoboken) *68*, 471–490.
6. De La Cruz, E.M. (2009). How cofilin severs an actin filament. Biophys. Rev. *1*, 51–59.
7. Elam, W.A., Kang, H., and De la Cruz, E.M. (2013). Biophysics of actin filament severing by cofilin. FEBS Lett. *587*, 1215–1219.
8. Suarez, C., Roland, J., Boujemaa-Paterski, R., Kang, H., McCullough, B.R., Reymann, A.C., Guérin, C., Martiel, J.L., De la Cruz, E.M., and Blanchoin, L. (2011). Cofilin tunes the nucleotide state of actin filaments and severs at bare and decorated segment boundaries. Curr. Biol. *21*, 862–868.
9. Okada, K., Obinata, T., and Abe, H. (1999). XAIP1: a Xenopus homologue of yeast actin interacting protein 1 (AIP1), which induces disassembly of actin filaments cooperatively with ADF/cofilin family proteins. J. Cell Sci. *112*, 1553–1565.
10. Rodal, A.A., Tetreault, J.W., Lappalainen, P., Drubin, D.G., and Amberg, D.C. (1999). Aip1p interacts with cofilin to disassemble actin filaments. J. Cell Biol. *145*, 1251–1264.
11. Okada, K., Blanchoin, L., Abe, H., Chen, H., Pollard, T.D., and Bamburg, J.R. (2002). Xenopus actin-interacting protein 1 (XAip1) enhances cofilin fragmentation of filaments by capping filament ends. J. Biol. Chem. *277*, 43011–43016.

molecules of ADF/cofilin are prone to an asymmetric severing event. After fragmentation, ADF/cofilin stretches remain near the pointed ends (PO), while barbed ends (BA) remain free to elongate. At a high concentration of ADF/cofilin (right), filaments decorated by stoichiometric densities of ADF/cofilin are stable. In this model, the conformation of actin filaments regulates the activity of Aip1. Only actin filaments decorated with N > 23 molecules of ADF/cofilin undergo a fast stochastic disassembly.

12. Rogers, S.L., Wiedemann, U., Stuurman, N., and Vale, R.D. (2003). Molecular requirements for actin-based lamella formation in Drosophila S2 cells. J. Cell Biol. *162*, 1079–1088.

13. Okada, K., Ravi, H., Smith, E.M., and Goode, B.L. (2006). Aip1 and cofilin promote rapid turnover of yeast actin patches and cables: a coordinated mechanism for severing and capping filaments. Mol. Biol. Cell *17*, 2855–2868.

14. Kato, A., Kurita, S., Hayashi, A., Kaji, N., Ohashi, K., and Mizuno, K. (2008). Critical roles of actin-interacting protein 1 in cytokinesis and chemotactic migration of mammalian cells. Biochem. J. *414*, 261–270.

15. Augustine, R.C., Pattavina, K.A., Tüzel, E., Vidali, L., and Bezanilla, M. (2011). Actin interacting protein1 and actin depolymerizing factor drive rapid actin dynamics in *Physcomitrella patens*. Plant Cell *23*, 3696–3710.

16. Chu, D., Pan, H., Wan, P., Wu, J., Luo, J., Zhu, H., and Chen, J. (2012). AIP1 acts with cofilin to control actin dynamics during epithelial morphogenesis. Development *139*, 3561–3571.

17. Chen, Q., Courtemanche, N., and Pollard, T.D. (2015). Aip1 promotes actin filament severing by cofilin and regulates constriction of the cytokinetic contractile ring. J. Biol. Chem. *290*, 2289–2300.

18. Nadkarni, A.V., and Brieher, W.M. (2014). Aip1 destabilizes cofilin-saturated actin filaments by severing and accelerating monomer dissociation from ends. Curr. Biol. *24*, 2749–2757.

19. Talman, A.M., Chong, R., Chia, J., Svitkina, T., and Agaisse, H. (2014). Actin network disassembly powers dissemination of Listeria monocytogenes. J. Cell Sci. *127*, 240–249.

20. Reymann, A.-C., Martiel, J.-L., Cambier, T., Blanchoin, L., Boujemaa-Paterski, R., and Théry, M. (2010). Nucleation geometry governs ordered actin networks structures. Nat. Mater. *9*, 827–832.

21. Rodal, A.A., Manning, A.L., Goode, B.L., and Drubin, D.G. (2003). Negative regulation of yeast WASp by two SH3 domain-containing proteins. Curr. Biol. *13*, 1000–1008.

22. Michelot, A., Costanzo, M., Sarkeshik, A., Boone, C., Yates, J.R., 3rd, and Drubin, D.G. (2010). Reconstitution and protein composition analysis of endocytic actin patches. Curr. Biol. *20*, 1890–1899.

23. Fujiwara, I., Takahashi, S., Tadakuma, H., Funatsu, T., and Ishiwata, S. (2002). Microscopic analysis of polymerization dynamics with individual actin filaments. Nat. Cell Biol. *4*, 666–673.

24. Kuhn, J.R., and Pollard, T.D. (2005). Real-time measurements of actin filament polymerization by total internal reflection fluorescence microscopy. Biophys. J. *88*, 1387–1402.

25. Michelot, A., Derivery, E., Paterski-Boujemaa, R., Guérin, C., Huang, S., Parcy, F., Staiger, C.J., and Blanchoin, L. (2006). A novel mechanism for the formation of actin-filament bundles by a nonprocessive formin. Curr. Biol. *16*, 1924–1930.

26. Balcer, H.I., Goodman, A.L., Rodal, A.A., Smith, E., Kugler, J., Heuser, J.E., and Goode, B.L. (2003). Coordinated regulation of actin filament turnover by a high-molecular-weight Srv2/CAP complex, cofilin, profilin, and Aip1. Curr. Biol. *13*, 2159–2169.

27. Cocucci, E., Aguet, F., Boulant, S., and Kirchhausen, T. (2012). The first five seconds in the life of a clathrin-coated pit. Cell *150*, 495–507.

28. Hayakawa, K., Sakakibara, S., Sokabe, M., and Tatsumi, H. (2014). Single-molecule imaging and kinetic analysis of cooperative cofilin-actin filament interactions. Proc. Natl. Acad. Sci. USA *111*, 9810–9815.

29. Andrianantoandro, E., and Pollard, T.D. (2006). Mechanism of actin filament turnover by severing and nucleation at different concentrations of ADF/cofilin. Mol. Cell *24*, 13–23.

30. Kueh, H.Y., Charras, G.T., Mitchison, T.J., and Brieher, W.M. (2008). Actin disassembly by cofilin, coronin, and Aip1 occurs in bursts and is inhibited by barbed-end cappers. J. Cell Biol. *182*, 341–353.

31. Tsuji, T., Miyoshi, T., Higashida, C., Narumiya, S., and Watanabe, N. (2009). An order of magnitude faster AIP1-associated actin disruption than nucleation by the Arp2/3 complex in lamellipodia. PLoS ONE *4*, e4921.

32. Michelot, A., Grassart, A., Okreglak, V., Costanzo, M., Boone, C., and Drubin, D.G. (2013). Actin filament elongation in Arp2/3-derived networks is controlled by three distinct mechanisms. Dev. Cell *24*, 182–195.

33. Ono, S., Mohri, K., and Ono, K. (2004). Microscopic evidence that actin-interacting protein 1 actively disassembles actin-depolymerizing factor/Cofilin-bound actin filaments. J. Biol. Chem. *279*, 14207–14212.

34. Okreglak, V., and Drubin, D.G. (2010). Loss of Aip1 reveals a role in maintaining the actin monomer pool and an in vivo oligomer assembly pathway. J. Cell Biol. *188*, 769–777.

35. Kaksonen, M., Sun, Y., and Drubin, D.G. (2003). A pathway for association of receptors, adaptors, and actin during endocytic internalization. Cell *115*, 475–487.

36. Moseley, J.B., and Goode, B.L. (2006). The yeast actin cytoskeleton: from cellular function to biochemical mechanism. Microbiol. Mol. Biol. Rev. *70*, 605–645.

37. Okreglak, V., and Drubin, D.G. (2007). Cofilin recruitment and function during actin-mediated endocytosis dictated by actin nucleotide state. J. Cell Biol. *178*, 1251–1264.

38. Kamasaki, T., Arai, R., Osumi, M., and Mabuchi, I. (2005). Directionality of F-actin cables changes during the fission yeast cell cycle. Nat. Cell Biol. *7*, 916–917.

39. Yu, J.H., Crevenna, A.H., Bettenbühl, M., Freisinger, T., and Wedlich-Söldner, R. (2011). Cortical actin dynamics driven by formins and myosin V. J. Cell Sci. *124*, 1533–1541.

40. Kamasaki, T., Osumi, M., and Mabuchi, I. (2007). Three-dimensional arrangement of F-actin in the contractile ring of fission yeast. J. Cell Biol. *178*, 765–771.

41. Mendes Pinto, I., Rubinstein, B., Kucharavy, A., Unruh, J.R., and Li, R. (2012). Actin depolymerization drives actomyosin ring contraction during budding yeast cytokinesis. Dev. Cell *22*, 1247–1260.

42. Stachowiak, M.R., Laplante, C., Chin, H.F., Guirao, B., Karatekin, E., Pollard, T.D., and O'Shaughnessy, B. (2014). Mechanism of cytokinetic contractile ring constriction in fission yeast. Dev. Cell *29*, 547–561.

43. Lappalainen, P., and Drubin, D.G. (1997). Cofilin promotes rapid actin filament turnover in vivo. Nature *388*, 78–82.

44. Reymann, A.-C., Boujemaa-Paterski, R., Martiel, J.-L., Guérin, C., Cao, W., Chin, H.F., De La Cruz, E.M., Théry, M., and Blanchoin, L. (2012). Actin network architecture can determine myosin motor activity. Science *336*, 1310–1314.

45. Blanchoin, L., Pollard, T.D., and Mullins, R.D. (2000). Interactions of ADF/cofilin, Arp2/3 complex, capping protein and profilin in remodeling of branched actin filament networks. Curr. Biol. *10*, 1273–1282.

46. Chan, C., Beltzner, C.C., and Pollard, T.D. (2009). Cofilin dissociates Arp2/3 complex and branches from actin filaments. Curr. Biol. *19*, 537–545.

47. Galkin, V.E., Orlova, A., VanLoock, M.S., Shvetsov, A., Reisler, E., and Egelman, E.H. (2003). ADF/cofilin use an intrinsic mode of F-actin instability to disrupt actin filaments. J. Cell Biol. *163*, 1057–1066.

48. Galkin, V.E., Orlova, A., Kudryashov, D.S., Solodukhin, A., Reisler, E., Schröder, G.F., and Egelman, E.H. (2011). Remodeling of actin filaments by ADF/cofilin proteins. Proc. Natl. Acad. Sci. USA *108*, 20568–20572.

49. Ngo, K.X., Kodera, N., Katayama, E., Ando, T., and Uyeda, T.Q. (2015). Cofilin-induced unidirectional cooperative conformational changes in actin filaments revealed by high-speed atomic force microscopy. eLife *4*, 1–22.

50. Reymann, A.-C., Guérin, C., Théry, M., Blanchoin, L., and Boujemaa-Paterski, R. (2014). Geometrical control of actin assembly and contractility. Methods Cell Biol. *120*, 19–38.